Hindawi
Advances in Materials Science and Engineering
Volume 2018, Article ID 2876851, 10 pages
https://doi.org/10.1155/2018/2876851

*Research Article*

# Porogenic Behavior of Water in High-Alumina Castable Structures

**Rafael Salomão**

*Materials Engineering Department, São Carlos School of Engineering, University of São Paulo, Avenida Trabalhador São-carlense 400, São Carlos, SP, Brazil*

Correspondence should be addressed to Rafael Salomão; rsalomao@sc.usp.br

Received 31 October 2017; Revised 30 January 2018; Accepted 26 April 2018; Published 7 June 2018

Academic Editor: Marino Lavorgna



Direct casting is a processing method that can produce large parts of complex geometry. It uses dispersions of ceramic particles in water and a hydraulic binder for consolidation. Studies on castable structures have reported the generation of a significant fraction of pores due to the presence of water. This effect occurs because drying preserves part of the interparticle pores originally occupied by water. The fraction of pores obtained in these cases can reach levels higher than 50%, affecting the properties of the structure. However, the porogenic behavior of water in these materials was not investigated in depth. In this work, aqueous suspensions of calcined alumina and hydratable alumina (hydraulic binder) of different water contents (40–60 vol.%) were prepared in a paddler mixer. For compositions of lower (5–35 vol.%) or higher (66–80 vol.%) water amounts, casting and curing steps were assisted by external pressure and a rotating device, respectively, to produce homogeneous microstructures. The total porosity after drying was similar to the initial volumetric content of water in the compositions when side effects, such as sedimentation and air entrapment, were prevented. Below water content of 25 vol.%, particles packing flaws became the main pore generator and the hydroxylation reaction of the binder no longer occurred effectively.

## 1. Introduction

In the process known as direct casting, ceramic particles are mixed with water, additives, and a binder to produce a stable suspension [1–5]. After homogenization, the system is cast into the desired shape and curing reactions harden the structure [6, 7]. The parts are then demolded and dried (in some cases, further steps of thermal treatment are required). Due to its straightforwardness, direct casting is widely used to produce large parts of concrete in civil construction [5] and pieces of complex shapes of refractory materials [3, 4, 6, 7] and recently has been used to produce porous structures for high-temperature thermal insulation [8–11]. Water is a key ingredient in such processes and plays three main roles.

Firstly, water wets the surface of ceramic particles forming a continuous phase amongst them (Figure 1(a)) [5, 12–15]. Stable suspensions containing high solid loads can be produced using particles of optimized size distribution, proper dispersants to prevent agglomeration, and suitable mixing of high shear and turbulence [16–20]. Under favorable conditions, such suspensions can present low viscosity and excellent workability, which are requirements to facilitate the casting step and prevent the undesired entrapment of air bubbles into the structure. Secondly, the presence of water generates strong capillarity forces amongst large and fine particles (Figure 1(b)) [17, 18, 20, 21]. Such forces are known as *Wall effect* and improve the packing efficiency of the system (compared to the same particle size distribution without water or application of external compacting forces). Thirdly, water is a major component of most binding systems for castable suspensions (Figure 1(c)) [22–25]. The reactions amongst water and hydraulic binders (such as Portland and calcium aluminate cements, hydratable alumina, and plaster) during mixing and curing steps produce hydrated compounds that restrain the matrix particle movement. Colloidal binders (such as aqueous suspensions of silica and alumina nanoparticles) and polymeric binders (chitosan and sodium alginate) work in a similar way hardening the structure [7, 19]. Because all these chemical reactions and the setting of the structures

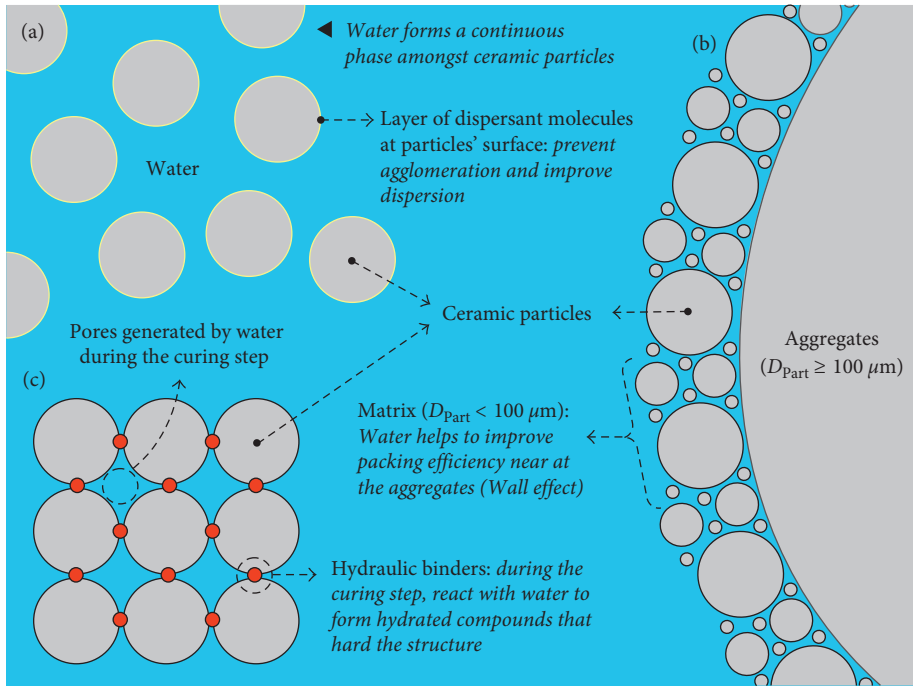


Figure 1: Roles of water in the preparation of ceramic particles suspensions: (a) it is a continuous medium for particle dispersion, (b) it improves particle packing through the Wall effect, and (c) it reacts with a hydraulic binder to strengthen the structure.

occur in the presence of water, most of the spaces it occupies during mixing are preserved during the curing and drying steps. As a consequence, direct casting usually produces structures of higher porosity than other consolidating methods (such as pressing and slip-casting) [21, 26].

This last aspect has been recently used as an advantageous way to produce porous ceramics. Aqueous suspensions of calcined alumina or silica (dense matrixes), several inorganic porogenic agents (hydrotalcite [8], $Al(OH)_3$ [9, 10], $Mg(OH)_2$ [27], and $CaCO_3$ [28]) and hydratable alumina were produced and directly cast using hydraulic binders (hydratable alumina, mainly). In these systems, the total porosity levels attained after curing and drying (50–120°C, 45–60%) were close to the volumetric amount of water initially added during mixing (40–55%). After thermal treatment (up to 1700°C), pore content increases occurred due to the dehydroxilation/decarbonatation of the porogenic agents and hydrated phases of the hydraulic binders. Therefore, the final total porosity levels of these castable suspensions can be defined as a contribution of pores formed by water during the setting period (Figure 1(c)) and by the decomposition of porogenic agents. Based on this statement, it is reasonable to assume that by controlling the water amount in the composition, the total porosity level of the structures can be designed.

For each system, there is an optimum amount of water to produce stable castable suspensions that can be determined by means of viscosity measurements. If the water content in the casting suspensions is excessive, particle sedimentation may occur. On the other hand, if the total water amount in the system is not enough to wet and spread particles, a continuous medium is not formed. In both cases, structures of low homogeneity are produced. To overcome these aspects and study the impact of a wide variation in the water content in physical properties of castable systems, the present study used two strategies: (1) to produce suspensions of very high solid loads (60–95 vol.%), water was added to the powders as a spray and the consolidation was assisted by isostatic pressing and (2) to prevent particle sedimentation, the initial setting of very low solid-load suspensions (20–55 vol.%) was performed in a rotating device that slightly agitates the liquid inside the molds before hardening. The samples prepared by these methods were compared to others produced in a conventional paddler mixer and static casting conditions (solid load varying from 20 up to 75 vol.%).

## 2. Experimental

Raw materials: calcined alumina (CA, E-sy 1000, Almatis, USA), hydratable alumina (HA, Alphabond 300, Almatis, USA), dispersant (diammonium citrate, $C_6H_{14}N_2O_7$, DAC, Synth, Brazil, 0.30 wt.% dry-basis), and distilled water (from 5 vol.% up to 80 vol.%) (Table 1). The optimum dispersant content was previously determined and was in good agreement with other reports [13].

Samples were prepared using three different casting and curing methods (Table 2). (1) Static curing: suspensions containing 25–80 vol.% of water were homogenized in a paddler mixer (PowerVisc, Ika, Germany, 1000 rpm for 5 minutes), cast under vibration as cylinders (length: 70 mm, diameter: 16 mm), and kept immobile at 60 ± 2°C for 24 h in high-humidity atmosphere. (2) Curing under rotation: after mixing and casting under vibration, the molds containing compositions of 45–80 vol.% of water were capped and fixed inside polyethylene spheres (diameter of 8 cm) placed

Table 1: Characteristics of the raw materials tested.

| Physic-chemical properties | Solid particles | |
|---|---|---|
| | Calcined alumina (CA) | Hydratable alumina (HA) |
| [a]Composition (wt.%) | $\alpha$-$Al_2O_3$: 99.7; $Na_2O$: 0.2; $Fe_2O_3$: 0.03; $SiO_2$: 0.34; CaO: 0.03 | $\alpha$-$Al_2O_3$: 99.4; $Na_2O$: 0.05; $Fe_2O_3$: 0.02; MgO: 0.07; $SiO_2$: 0.03; CaO: 0.02 |
| [b]Particles size ($D_{50}/D_{90}$, $\mu$m) | 1.5/9.6 | 7.6/31 |
| [c]Solid density ($\rho$, g·cm$^{-3}$) | 3.89 | 2.72 |
| [d]Specific surface area (SSA, $m^2 \cdot g^{-1}$) | 1.3 | 95 |
| [e]LOI (wt.%, 1000°C) | <0.1 | 8.2 |

[a]X-ray dispersive spectroscopy (EDX 720, Shimadzu, Japan, after calcination at 1000°C for 5 h). [b]DT-1202 (Dispersion Technology Inc., USA). [c]Helium pycnometer method (Ultrapyc 1200e, Quantachrome Instruments, USA). [d]$N_2$ adsorption (Nova 1200e, Quantachrome Instruments, USA, ASTM C 1069-09 standard). [e]Thermogravimetry (TGA-Q50, TA Instruments, 25–1000°C, 5°C·min$^{-1}$ heating rate and synthetic air atmosphere).

Table 2: Tested compositions.

| Casting and curing methods | Raw materials (vol.%/wt.%) | | | |
|---|---|---|---|---|
| | Water ($W$) | Calcined alumina (CA) | Hydratable alumina (HA) | Solids load (CA + HA) |
| Under pressure | 5.00/1.34 | 85.50/91.71 | 9.50/6.95 | 95.00/98.66 |
| Under pressure | 10.00/2.80 | 81.00/90.36 | 9.00/6.84 | 90.00/97.20 |
| Under pressure | 15.00/4.37 | 76.50/88.90 | 8.50/6.73 | 85.00/95.63 |
| Under pressure | 20.00/6.08 | 72.00/87.31 | 8.00/6.61 | 80.00/93.92 |
| Under pressure, static | 25.00/7.94 | 67.50/85.57 | 7.50/6.48 | 75.00/92.06 |
| Under pressure, static | 30.00/9.99 | 63.00/83.68 | 7.00/6.34 | 70.00/90.01 |
| Under pressure, static | 35.00/12.23 | 58.50/81.59 | 6.50/6.18 | 65.00/87.77 |
| Under pressure, static | 40.00/14.72 | 54.00/79.28 | 6.00/6.00 | 60.00/85.28 |
| Static, under rotation | 45.00/17.48 | 49.50/76.71 | 5.50/5.81 | 55.00/82.52 |
| Static, under rotation | 50.00/20.56 | 45.00/73.84 | 5.00/5.59 | 50.00/79.44 |
| Static, under rotation | 55.00/24.03 | 40.50/70.62 | 4.50/5.35 | 45.00/75.97 |
| Static, under rotation | 60.00/27.97 | 36.00/66.96 | 4.00/5.07 | 40.00/72.03 |
| Static, under rotation | 65.00/32.47 | 31.50/62.78 | 3.50/4.76 | 35.00/67.53 |
| Static, under rotation | 70.00/37.66 | 27.00/57.95 | 3.00/4.39 | 30.00/62.34 |
| Static, under rotation | 75.00/43.71 | 22.50/52.32 | 2.50/3.96 | 25.00/56.29 |
| Static, under rotation | 80.00/50.87 | 18.00/45.67 | 2.00/3.46 | 20.00/49.13 |

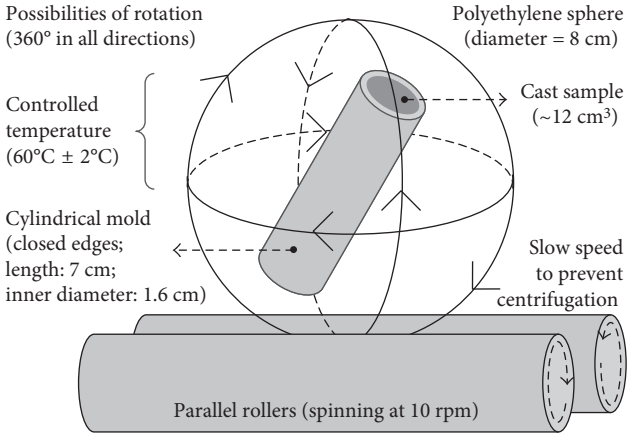


Figure 2: Rotating device used to prevent particle sedimentation during the curing step of very low solid-load suspensions.

between two corotating cylinders (10 rpm) at 60 ± 2°C (Figure 2). In such an arrangement, these spheres can rotate freely in all directions, and the gentile movement of the suspensions inside the molds prevents particle sedimentation. After 2 h, all compositions were rigid and remained static for another 22 h at 60 ± 2°C in high-humidity atmosphere. (3) Casting under pressure: to produce samples of a very high solid load, water (5–40 vol.%) was sprayed over the solid particles previously dry-mixed. Afterwards, these humid mixtures were homogenized in an intensive stirrer (IKA1603600, IKA, Germany) and compacted as 70 mm × 16 mm cylinders by isostatic pressing (Trexler CP360, USA, 5 MPa, 60 s), using flexible silicone molds. Then, the samples were kept immobile at 60 ± 2°C for 24 h in high-humidity atmosphere. A water-free reference sample was prepared using the same method.

After the initial 24 h of curing, all samples were demolded and remained 24 h at 60 ± 2°C and 24 h at 120 ± 4°C in a ventilated atmosphere. These curing procedures were used to maximize the binding effect of HA and reduce the likelihood of explosive spalling during the first drying [6, 10, 22, 23].

Samples were measured ($L$, length; $D$, diameter) and weighted ($M$, mass) immediately after demolding (humid stage, HS) and after drying at 120°C (dried stage, DS). Their linear shrinkage after drying (LS, %) was calculated using

$$\mathrm{LS} = 100\% \times \left[\frac{(L_{\mathrm{HS}} - L_{\mathrm{DS}})}{L_{\mathrm{HS}}}\right]. \quad (1)$$

The total porosity (TP, %) of the dried samples was calculated using

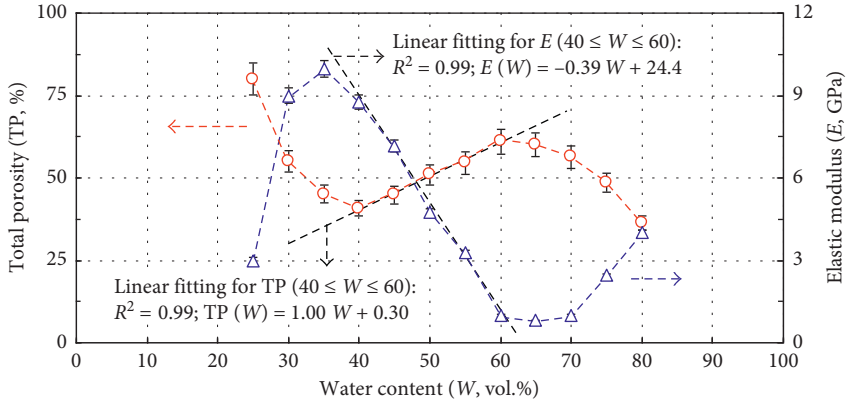


FIGURE 3: Effects of water content ($W$ vol.%) on samples' total porosity (TP, %) and flexural elastic modulus ($E$ GPa) after conventional static curing and drying at 120°C for 24 h.

$$\mathrm{TP} = 100\% \times \left[1 - \left(\frac{4 \cdot M_{DS}}{\pi \cdot D_{DS}^2 \cdot L_{DS} \cdot \rho_{Solid}}\right)\right]. \quad (2)$$

where $\rho_{Solid}$ is the solid density of the material (measured by He pycnometer method in equivalent crushed samples).

The Young's modulus ($E$, GPa) of dried samples was measured using impulse excitation of the vibration technique (Sonelastic, ATCP, Brazil), according to the ASTM E 1876-01 standard ("Standard Test Method for Dynamic Young's Modulus, Shear Modulus, and Poisson's Ration by Impulse Excitation of Vibration"). Each linear shrinkage, total porosity, and elastic modulus result is the average value of five different samples.

Samples' pore size distributions and average pore size (APS) were determined by mercury intrusion porosimetry (PoreMaster 33, Quantochrome Instruments, USA; mercury surface tension equal to 0.480 $\mathrm{N{\cdot}m^{-1}}$; contact angle of 130°) and ranging applied pressure between 0.0014 and 210 MPa. The fractures' cross sections of the samples were examined by field emission scanning electron microscopy (FEG-SEM).

To understand how the workability of the suspensions can affect particle packing and other physical properties, the apparent viscosity of the suspensions (30–80 vol.% of water) was measured (Brookfield Viscosimeter, VLDV-II+PRO, USA) using a coaxial cylinder configuration (barrel: 19 mm diameter by 65 mm length and spindle 17.47 mm diameter by 31.85 mm height). During the measurements (at a shear rate of 50 $\mathrm{s^{-1}}$ for 60 seconds), the temperature of the suspensions was kept at 25°C ± 0.5°C (thermal bath, Brookfield TC-550, USA). These parameters were previously determined as sufficient to achieve steady-state conditions. The shear rate of 50 $\mathrm{s^{-1}}$ was chosen because the casting techniques that could be used to install this system usually employ shear rates of 10–100 $\mathrm{s^{-1}}$.

## 3. Results and Discussion

*3.1. Conventional Processing: Suspensions Homogenized in Paddler Mixer and Cured Statically.* Samples' total porosity (TP) presented a strong linear dependence on water content at the interval from 40 vol.% up to 60 vol.% (Figure 3). In this range, the TP values were very close to the initial volumetric amount of water in the composition. It is noteworthy that the water amount affected pores' size distribution (Figure 4) and morphology (Figures 5(a) and 5(b)). This behavior occurs because during the setting period of the binder, the greater the water content in the formulation, the more apart particles are in the suspension. Consequently, as average space amongst the particles in suspension increases, TP and average pore size enhance linearly. Although the morphology of the pores remained irregular, it was possible to observe a significant reduction in the particles' packing efficiency. Such behaviors are typical from cast systems containing hydraulic binders such as hydratable alumina [6, 7, 10, 29]. On the other hand, further increasing or decreasing in the water content beyond or below this range, respectively, resulted in the opposite behavior, with significant deviations of linearity. These unusual behaviors can be understood analyzing the processing conditions.

Suspensions of water contents below 40 vol.% presented high levels of apparent viscosity ($\eta$, Figure 6) due to two mains effects. Firstly, for a same solid-liquid pair, low water contents generate denser fluids that require greater energy to be deformed and flow [12, 15, 16]. Therefore, the denser the suspensions, the higher their apparent viscosity levels and vice-versa. Secondly, the high solid load reduces significantly the spacing amongst particles and forms narrow channels of nanometric dimension through which water must flow [17, 18]. Due to this, the strong capillarity and attrite forces and the constant shocks generated amongst particles restrain their movement. The usually undesired consequence of the high viscosity is the entrapment of air bubbles during the mixing that increases the porosity of the structure well above the volumetric water content in the composition. Figures 7(a) and 7(b) presents the aspect of such samples at which large millimetric voids are visible at the surface and beneath it in comparison to a defect-free one.

Conversely, suspensions of high water content (above 60 vol.%) exhibited very low apparent viscosity levels and a linear dependence on the water content in the range of 40–80 vol.%. This effect was reported elsewhere and is also explained by means of the increase in the average spacing

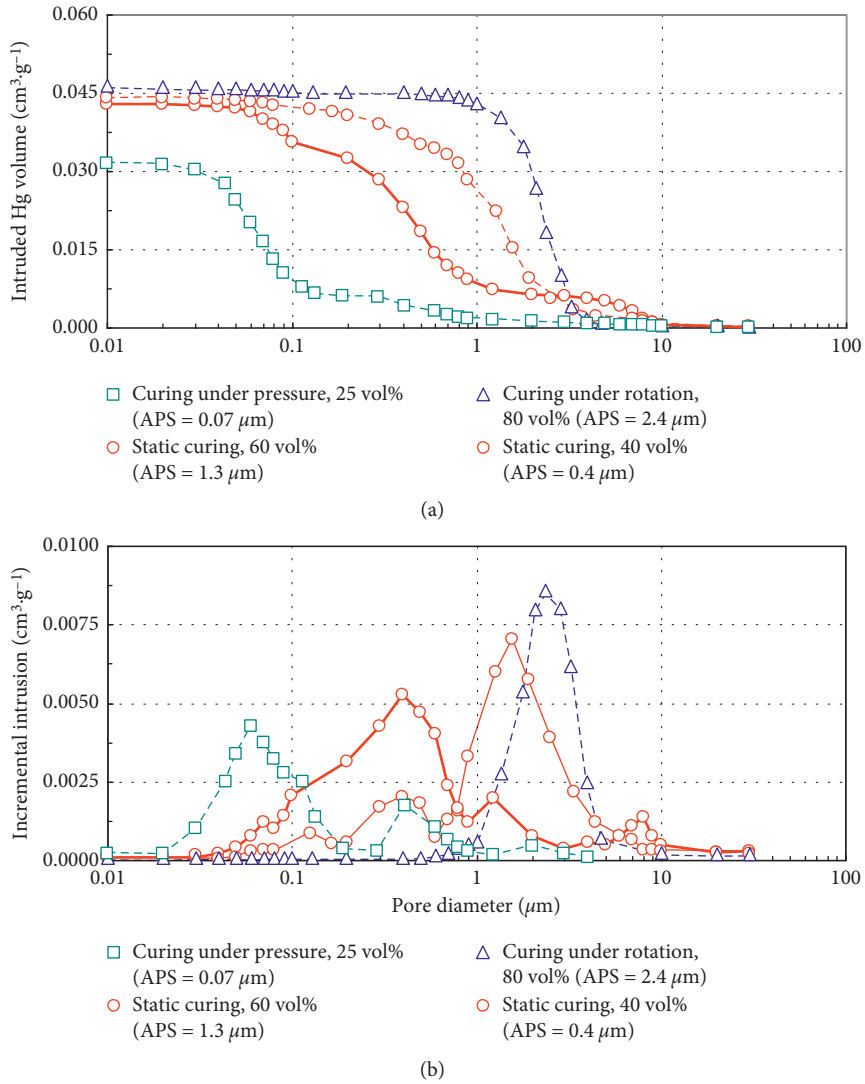


Figure 4: (a) Continuous and (b) incremental pore size distribution for samples mixed and cured in the conventional static way containing 40 vol.% and 60 vol.% of water, containing 80 vol.% of water after curing under rotation, and containing 25 vol.% of water cast under isostatic pressing. APS = average pore size.

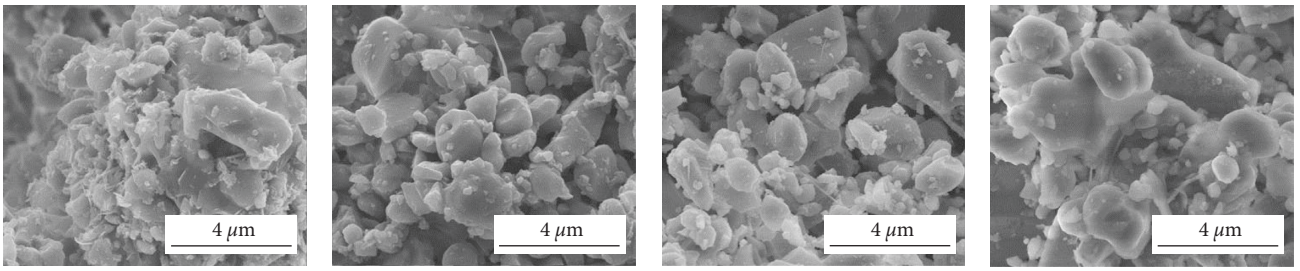


Figure 5: Microstructure of sample samples mixed and cured in the conventional static way containing (a) 40 vol.% and (b) 60 vol.% of water, (c) containing 80 vol.% of water after curing under rotation, (d) and containing 25 vol.% of water cast under isostatic pressing.

amongst particles and of the reduction in the whole density of the suspension [12, 17, 18]. Despite the easy mixing and casting, the intense shrinkage observed after drying (Figure 6) is a harmful side effect. In these suspensions, the excess of water reduced the binding effect of hydratable alumina and favored particle sedimentation

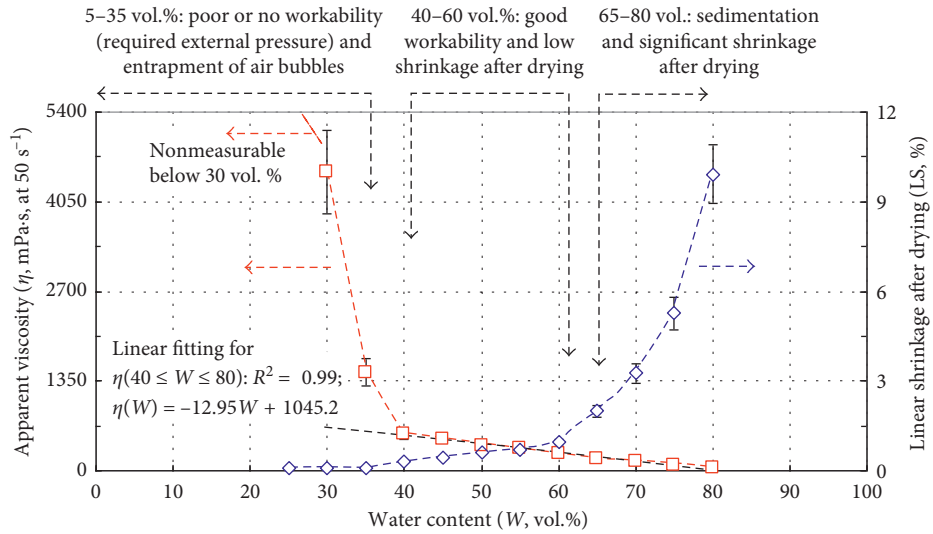


FIGURE 6: Effects of water content ($W$ vol.%) on compositions' apparent viscosity ($\eta$, mPa·s$^{-1}$, measured at 50 s$^{-1}$ and 25°C) and linear shrinkage after drying (LS, %, after 24 h at 120°C, for samples cured in the conventional static way).

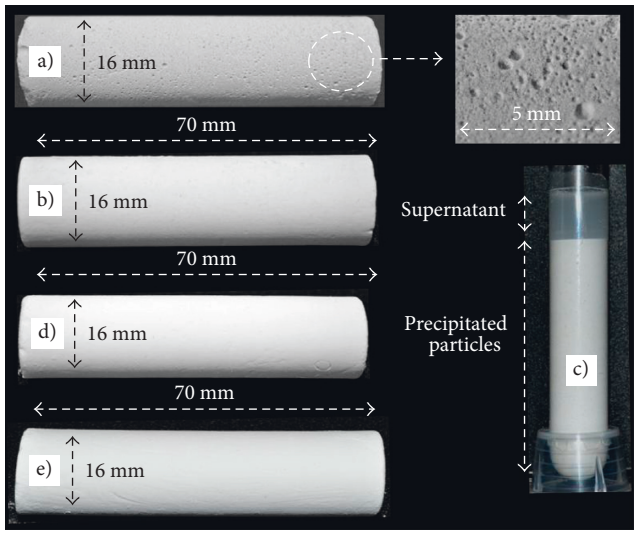


FIGURE 7: Samples mixed and cured in the conventional static way containing (a) 25 vol.%, (b) 50 vol.%, and (c) 80 vol.% of water (tube containing sedimented suspension); (d) sample containing 80 vol.% of water after curing under rotation; (e) sample containing 25 vol.% of water cast under isostatic pressing.

during the curing step (Figure 5(c)). Therefore, as the particles were practically free to move around, during the drying step, the water withdrawal shrank the samples reducing their total porosity. Other processing methods (such as slip-casting) use this mechanism to improve particle packing and to produce dense structures. In direct casting, on the other hand, the poor dimension control and the generation of cracks are significant drawbacks that must be avoided.

The effects of water content and, consequently, pore generation upon samples' flexural elastic modulus are shown in Figure 3. As observed for TP, E presented an interval of linear dependency on the water amount (40–60 vol.%) and different behaviors for lower and higher contents. The linear range can be understood using a simple model known as *Rule of the Mixtures* [30]. For a composite consisting of $n$ different components, an estimate of its elastic modulus ($E_{\text{Composite}}$) can be calculated by the sum of each individual modulus value ($E_i$) multiplied by the correspondent volumetric fraction:

$$E_{\text{Composite}} = \sum_{1}^{n} (E_i \times \varnothing_i). \tag{3}$$

For a porous structure, the elastic modulus of the voids equals zero and (3) can be rewritten as a function of the elastic modulus and volumetric fraction of the dense part ($E_{\text{Dense}}$ and $\varnothing_{\text{Dense}}$, resp.):

$$E_{\text{Porous}} = (E_{\text{Dense}} \times \varnothing_{\text{Dense}}). \tag{4}$$

Unlike more sophisticated models, Rule of Mixtures is a simplification of the real case because it does not consider micromechanic effects, such as the effectiveness of the connections amongst particles and average pore sizes and shapes. Nevertheless, it explains the influence of TP on E levels quite well in the linear range. For water contents lower than 40 vol.% and greater than 60 vol.%, the E values drop and rise, respectively, following the TP level: the less porous the structure, the more rigid it becomes and vice-versa [5].

*3.2. Samples Cured under Rotation and under Isostatic Pressing.* The procedure of curing under rotation prevented particle sedimentation (Figure 7(d)) and reduced drying shrinkage (Figure 8(a)) significantly in all the water content ranges tested (45–80 vol.%). These effects indicate that the structure formed during curing, comprised by particles highly spaced amongst each other, was preserved by the binding effect of hydratable alumina. They also explain why TP levels became linearly similar to the initial volumetric water amount in these compositions after drying (Figure 8(b))

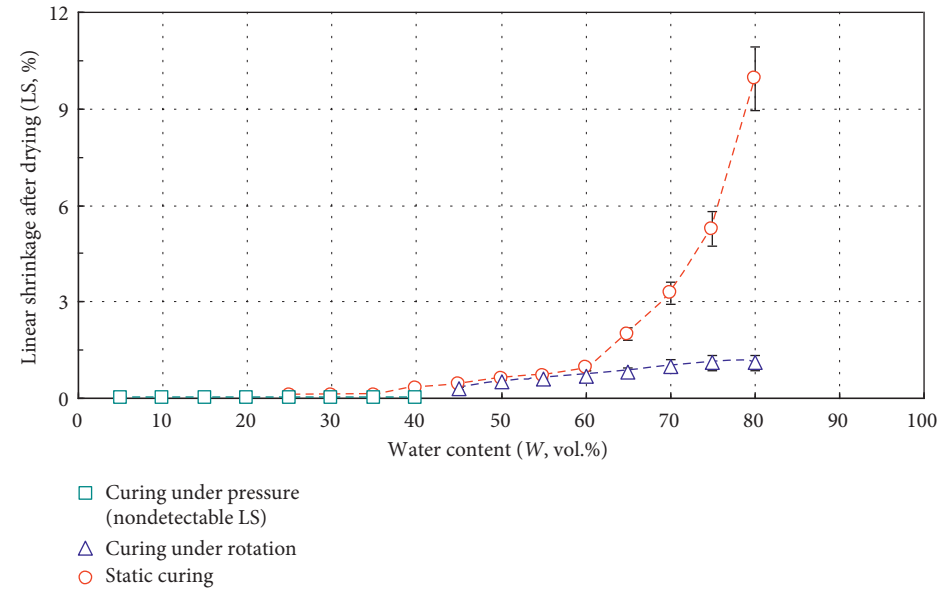


(a)

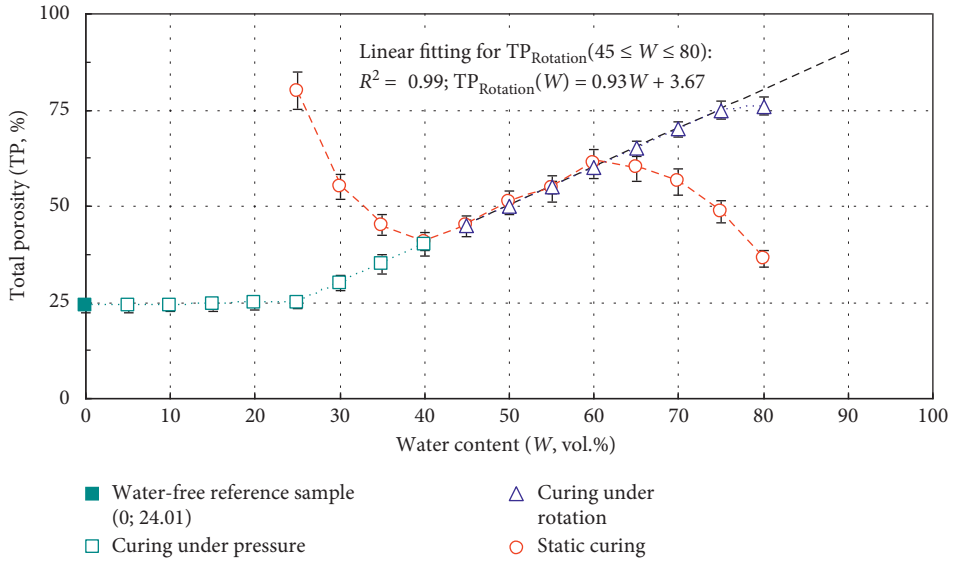


(b)

Figure 8: Continued.

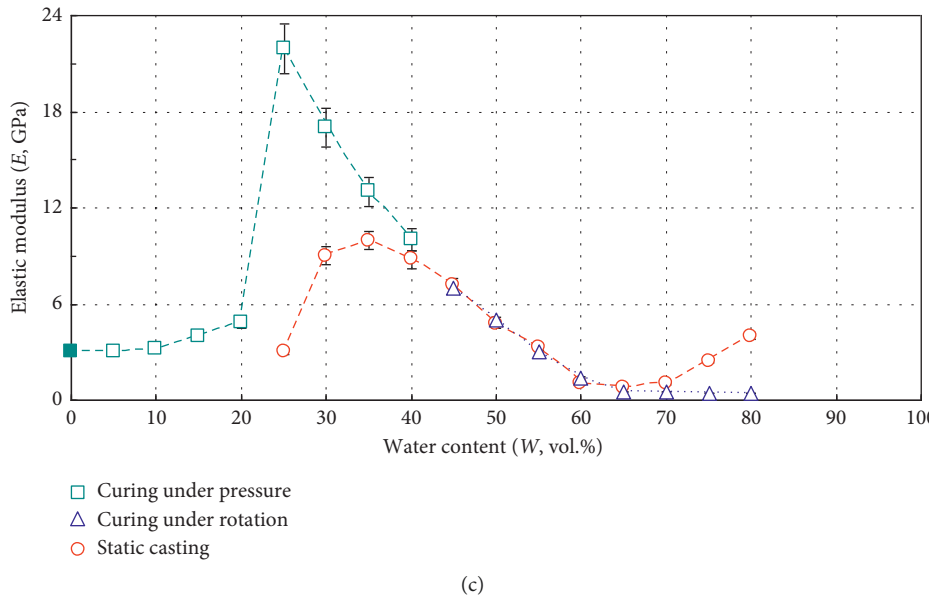


(c)

FIGURE 8: Effects of water content (*W* vol.%) on samples (a) linear shrinkage after drying (LS, %), (b) total porosity (TP, %), and (c) flexural elastic modulus (*E* GPa) after conventional static curing, curing under rotation, and curing under isostatic pressure (drying performed at 120°C for 24 h).

and the increase in the average pore size (Figure 4). The elastic modulus values, on the other hand, were drastically reduced as would be expected (the four smallest levels were ranged between 0.50 and 0.45 GPa) (Figure 8(c)), due to the large fraction of pores in the structures and the poor interconnections amongst the particles (Figure 5(c)).

Such very low levels of E for samples of TP greater than 50% are certainly a problem for materials that depend exclusively on the strengthening effect of the hydraulic binders. Concrete and mortar used in civil construction would require strategies to improve mechanical properties, such as fibers or steel bar reinforcement [5]. On the other hand, for systems that are thermally treated after curing and drying (such as high-temperature thermal insulators, e.g.), a significant gain of strength is expected after sintering and the high total porosity levels would be a technological advantage [26–28, 31].

Compared to samples prepared by conventional static curing, those cured under pressure presented no detectable shrinkage after drying (Figures 7(e) and 8(a)), significantly lower TP values (Figure 8(b)), and average pore size (Figure 4). These effects relate to the high efficiency of particle packing this shaping method produces (Figure 5(c)) and to the extremely low volume of water added to the compositions. In the water content range of 25–40 vol.%, the TP reduction generated a huge gain of rigidity (Figure 8(c)) at which the greatest E value is two times higher than the best result achieved for conventional processing and almost three times than those cured under rotation. These results suggest that for applications where the initial green strength is mandatory, curing under isostatic pressure could be a suitable alternative to adding larger amounts of binders.

For water contents below 25 vol.%, samples' TP values stabilize around 25%, and E levels are significantly reduced. To understand these effects, it is important to observe the behavior of the water-free reference sample. Because no water was added to this composition, the TP value attained after compacting relates to the pores generated by packing flaws amongst the particles (24.8%). This residual porosity could be reduced by means of changing the particle size distribution of the calcined alumina matrix [16, 17], but these points are beyond the scopus of the present study. On the other hand, the rigidity of these samples is a combination of the binding action of hydratable alumina and particle packing [6, 10, 16, 18]. The fact that the rigidity of the low water content samples is similar to the water-free one shows the low effectiveness of the hydraulic binder in such compositions. A possible explanation for that is that there was no enough water in the system to promote full hydroxylation of hydratable alumina [23–25].

## 4. Conclusions

Water can be a powerful porogenic agent for high-alumina structures consolidated by direct casting. In these materials, changing the volumetric amount of water in the composition directly affected the physical properties of the structure attained. When a conventional paddler mixer was used for homogenization, there was an intermediate water content range (40–60 vol.%) at which the suspensions produced presented good workability (low apparent viscosity and no significant sedimentation) and low drying shrinkage. In this range, the total porosity, average pore size, and flexural elastic modulus measured after drying presented a strong linear dependency on the original water content. When the water contents were excessively increased or reduced, processing drawbacks occurred. In the diluted suspensions (65–80 vol.% of water), particle sedimentation occurred and

structures of low homogeneity and high drying shrinkage were generated. For the more concentrated ones (5–35 vol.% of water), on the contrary, the poor workability promoted excessive entrapment or air bubbles increasing total porosity and reducing elastic modulus. The rotating device used to prevent particle sedimentation allowed the casting and curing of compositions containing up to 80 vol.% of water without segregation. For these samples, total porosity values were close to the original volumetric amount of water in the formulation, and their drying shrinkage was significantly reduced compared to conventional processing. Samples cured under isostatic compression and containing water amounts between 25 and 40 vol.% were the strongest amongst all the compositions tested because of their low total porosity and effective binding action of hydratable alumina. Additional water content reductions (0–20 vol.), on the contrary, did not further decrease the pore content. This behavior can be explained by the interparticle packing flaws intrinsically present in this system that became the main pore generator. Besides this, it is possible that the small quantity of water present in these samples was not enough to fully hydroxilate the hydratable alumina, reducing its binding effect.

## Conflicts of Interest

The authors declare that they have no conflicts of interest.

## Acknowledgments

Brazilian Research Foundations FAPESP (2010-19274-5) and CNPq (455861/2014-5) for supporting this study, and Almatis (Brazil, USA and Germany) for kindly supplying samples of calcined and hydratable aluminas.

## References

[1] G. V. Givan, L. D. Hart, and G. McZura, "Curing and firing high purity calcium aluminate-bonded tabular alumina castables," *American Ceramic Society Bulletin*, vol. 54, no. 8, pp. 710–713, 1975.

[2] A. Nishikawa, "Manufacture and properties of monolith refractories," in *Technology of Monolithic Refractories*, Plibrico Co. Ltd., Tokyo, Japan, 1984.

[3] W. E. Lee and R. E. Moore, "Evolution of *in situ* refractories in the 20th century," *Journal of the American Ceramic Society*, vol. 81, no. 6, pp. 1385–1410, 1998.

[4] F. A. Cardoso, M. D. M. Innocentini, M. M. Akiyoshi, and V. C. Pandolfelli, "Effect of curing time on the properties of CAC bonded refractory castables," *Journal of the European Ceramic Society*, vol. 24, no. 7, pp. 2073–2078, 2004.

[5] P. K. Mehta and P. J. M. Monteiro, *Concrete: Microstructure, Properties, and Materials*, McGraw-Hill, New York, NY, USA, 3rd edition, 2006.

[6] R. Salomão, M. R. Ismael, and V. C. Pandolfelli, "Hydraulic binders for refractory castables: mixing, curing and drying," *Ceramic Forum International*, vol. 84, pp. E103–E108, 2007.

[7] M. R. Ismael, R. Salomão, and V. C. Pandolfelli, "Refractory castables based on colloidal silica and hydratable alumina," *American Ceramic Society Bulletin*, vol. 86, no. 9, pp. 58–61, 2007.

[8] R. Salomão, M. O. C. Villas-Boas, and V. C. Pandolfelli, "Porous alumina-spinel ceramics for high temperature applications," *Ceramics International*, vol. 37, no. 4, pp. 1393–1399, 2011.

[9] A. D. V. Souza, C. C. Arruda, L. Fernandes, M. L. P. Antunes, P. K. Kiyohara, and R. Salomão, "Characterization of aluminum hydroxide ($Al(OH)_3$) for its use as a porogenic agent in castable ceramics," *Journal of the European Ceramic Society*, vol. 35, no. 2, pp. 803–812, 2015.

[10] A. D. V. Souza, L. L. Sousa, L. Fernandes, P. H. L. Cardoso, and R. Salomão, "$Al_2O_3$-$Al(OH)_3$-based castable porous structures," *Journal of the European Ceramic Society*, vol. 35, no. 6, pp. 1943–1954, 2015.

[11] L. L. Sousa, A. D. V. Souza, L. Fernandez, V. L. Arantes, and R. Salomão, "Development of densification-resistant castable porous structures from *in situ* mullite," *Ceramics International*, vol. 41, no. 8, pp. 9943–9545, 2015.

[12] G. Schramm, *A Practical Approach to Rheology and Rheometry*, Gebrueder HAAKE GmbH, Karlsruhe, Germany, 2nd edition, 2000.

[13] A. R. Studart, V. C. Pandolfelli, E. Tervoot, and L. J. Gauckler, "Gelling of alumina suspensions using alginic acid salt and hydroxyaluminum diacetate," *Journal of the American Ceramic Society*, vol. 85, no. 11, pp. 2711–2718, 2002.

[14] F. T. Ramal, R. Salomão, and V. C. Pandolfelli, "Water content and its effect on the drying behavior of refractory castables," *Refractories Applications and News*, vol. 10, no. 3, pp. 10–17, 2005.

[15] F. S. Ortega, R. H. R. Castro, D. Gouvêa, and V. C. Pandolfelli, "The rheological behavior and surface charging of gelcasting alumina suspensions," *Ceramics International*, vol. 34, no. 1, pp. 237–241, 2008.

[16] D. M. Roy, B. C. Schutz, and M. R. Silsbee, "Processing and optimized cements and concretes via particle packing," *Materials Research Society Bulletin*, vol. 18, no. 3, pp. 45–49, 1993.

[17] J. E. Funk and D. R. Dinger, *Predictive Process Control of Crowded Particle Suspensions Applied to Ceramics Manufacturing*, Kluwer Academic Publishers, England, 1994.

[18] J. E. Funk and D. R. Dinger, "Particle size control for high-solids castables refractories," *American Ceramic Society Bulletin*, vol. 73, no. 10, pp. 66–69, 1994.

[19] M. R. Ismael, R. Salomão, and V. C. Pandolfelli, "Optimization of the particle size distribution of colloidal silica containing refractory castables," *Interceram*, vol. 4, pp. 34–39, 2007.

[20] R. Salomão and V. C. Pandolfelli, "The PSD effect on the drying efficiency of polymeric fibers containing castables," *Ceramics International*, vol. 34, no. 1, pp. 173–180, 2008.

[21] J. P. Ollivier, J. C. Maso, and B. Bourdette, "Interfacial transition zone in concrete," *Advanced Cement Based Materials*, vol. 2, no. 1, pp. 30–38, 1995.

[22] W. Ma and P. W. Brown, "Mechanisms of reaction of hydratable aluminas," *Journal of the American Ceramic Society*, vol. 82, no. 2, pp. 453–456, 1999.

[23] F. A. Cardoso, M. D. M. Innocentini, M. F. Miranda, F. A. O. Valenzuela, and V. C. Pandolfelli, "Drying behavior of hydratable alumina-bonded refractory castables," *Journal of the European Ceramic Society*, vol. 24, no. 5, pp. 797–802, 2004.

[24] I. R. Oliveira and V. C. Pandolfelli, "Castable matrix, additives and their role on hydraulic binder hydration," *Ceramics International*, vol. 35, no. 4, pp. 1453–1460, 2009.

[25] R. Salomão and V. C. Pandolfelli, "The role of hydraulic binders on magnesia containing refractory castables: calcium aluminate cement and hydratable alumina," *Ceramics International*, vol. 35, no. 8, pp. 3117–3124, 2009.

[26] A. D. V. Souza and R. Salomão, "Evaluation of the porogenic behavior of aluminum hydroxide particles of different size distribution in castable high-alumina structures," *Journal of the European Ceramic Society*, vol. 36, no. 3, pp. 885–897, 2016.

[27] R. Salomão, A. D. V. Souza, and P. H. L. Cardoso, "A comparison of $Al(OH)_3$ and $Mg(OH)_2$ as inorganic porogenic agents for alumina," *Interceram–Refractories Manual*, vol. 4, pp. 193–199, 2015.

[28] R. Salomão, V. L. Ferreira, I. R. Oliveira, A. D. V. Souza, and W. R. Correr, "Mechanism of pore generation in calcium hexaluminate ($CA_6$) ceramics formed in situ from calcined alumina and calcium carbonate aggregates," *Journal of the European Ceramic Society*, vol. 36, no. 16, pp. 4225–4235, 2016.

[29] R. Salomão, M. A. Kawamura, A. D. V. Souza, and J. Sakihama, "Hydratable alumina-bonded suspensions: evolution of microstructure and physical properties during first heating," *Interceram–Refractories Manual*, vol. 1, pp. 28–23, 2017.

[30] H. Ledbetter, S. Kim, D. Balzar, S. Crudele, and W. Kriven, "Elastic properties of mullite," *Journal of the American Ceramic Society*, vol. 81, no. 4, pp. 1025–1028, 1998.

[31] A. R. Studart, U. T. Gonzenbach, E. Tervoot, and L. J. Gauckler, "Processing routes to macroporous ceramics: a review," *Journal of the American Ceramic Society*, vol. 89, no. 6, pp. 1771–1789, 2006.